Causal Links Between Arctic Sea Ice and Its Potential Drivers Based on the Rate of Information Transfer

D. Docquier[1] , S. Vannitsem[1] , F. Ragone[1,2] , K. Wyser[3] , and X. S. Liang[4]

[1]Royal Meteorological Institute of Belgium, Brussels, Belgium, [2]Université catholique de Louvain, Louvain-la-Neuve, Belgium, [3]Rossby Centre, Swedish Meteorological and Hydrological Institute, Norrkoping, Sweden, [4]Fudan University, Shanghai, China

Abstract Arctic sea ice has substantially changed over the past four decades, with a large decrease in sea-ice area and volume. The exact causes of these changes are not entirely known. In our study, we make use of the Swedish Meteorological and Hydrological Institute Large Ensemble. This ensemble consists of 50 members realized with the EC-Earth3 global climate model and covers the period 1970-2100. We apply for the first time the Liang-Kleeman information flow method to analyze the cause-effect relationships between Arctic sea ice and its potential drivers. We show that recent and future changes in Arctic sea ice are mainly driven by air and sea-surface temperatures and ocean heat transport. Conversely, changes in Arctic sea ice also considerably impact temperature and ocean heat transport. Finally, we find a progressive decrease in the influence of sea-ice area and volume on air temperature and ocean heat transport through the twenty-first century.

Plain Language Summary The Arctic has been warming at a larger rate than the rest of the world, resulting in a substantial loss of sea ice since the late 1970s. This has had and will continue to have an impact on our climate and societies. The exact causes of the ongoing sea-ice loss are not entirely known, and understanding them is important in order to better prepare our societies for future climate changes. In our study, we apply a relatively novel approach that quantifies the cause-effect relationships between Arctic sea ice and its potential drivers. We make use of a large range of model simulations performed with the EC-Earth3 global climate model covering the period 1970-2100. We find that air temperature, sea-surface temperature, and the transport of heat by the ocean are important drivers of the ongoing and future retreat of Arctic sea ice. Conversely, changes in Arctic sea ice also affect the three former quantities. Our study demonstrates the performance of causal inference methods in the quest for a better understanding of relationships between climate variables. The geophysical and climate communities could greatly benefit from using these methods more intensively.

1. Introduction

Arctic sea ice has been retreating and thinning since the beginning of satellite observations in the late 1970s. Arctic sea-ice area, defined as the total area of the Arctic Ocean covered by sea ice, has decreased by ~2 million km^2 (in annual mean) since 1979, with stronger loss in summer compared to winter (IPCC, 2019; Onarheim et al., 2018; Stroeve & Notz, 2018). As sea ice has also been thinning (Kwok, 2018; Lindsay & Schweiger, 2015), the annual mean Arctic sea-ice volume has decreased by ~12,000 km^3 since 1979 (Schweiger et al., 2019). Model projections show a more or less rapid continuation of this ongoing process depending on the greenhouse gas emission scenario, with likely summer ice-free Arctic conditions (September Arctic sea-ice area lower than 1 million km^2) occurring before 2050 (Arthun et al., 2021; Docquier & Koenigk, 2021; SIMIP Community, 2020).

Recent changes in Arctic sea ice have been linked to both anthropogenic global warming (Notz & Stroeve, 2016) and climate internal variability (Swart et al., 2015). However, the exact drivers influencing sea-ice loss and their respective contributions are not fully understood. Both atmospheric (Ding et al., 2017) and ocean (Carmack et al., 2015) processes play a role in Arctic sea-ice changes. Typically, changes in near-surface air temperature strongly control the variability in Arctic sea-ice area over short time scales (Olonscheck et al., 2019), while ocean heat transport has a stronger impact on longer time scales (Onarheim et al., 2015).

The influence of atmospheric and ocean processes on Arctic sea ice is usually quantified via correlation and regression analyses, including or not a lag (Arthun et al., 2012; Auclair & Tremblay, 2018; Sando et al., 2014).

Visualization: D. Docquier, S. Vannitsem
Writing – original draft: D. Docquier,
S. Vannitsem, F. Ragone, K. Wyser, X.
S. Liang
Writing – review & editing: D.
Docquier, S. Vannitsem, F. Ragone, K.
Wyser, X. S. Liang

However, the presence of a correlation between one variable and another does not firmly demonstrate a causal influence between these variables. In order to identify such a causal link, causal inference frameworks can be used (Granger, 1969; Krakovska et al., 2018; Liang, 2014; Runge et al., 2019; Sugihara et al., 2012) and have been applied to climate studies (e.g., Deza et al., 2015; Harries & O'Kane, 2021; Kretschmer et al., 2016; Mosedale et al., 2006; Tsonis et al., 2015; Vannitsem & Ekelmans, 2018). The Liang-Kleeman information flow method (Liang & Kleeman, 2005) is particularly interesting because it allows identifying of the direction and magnitude of the cause-effect relationships between variables (Liang, 2014, 2021). This novel method has been successfully applied to several climate studies, for example, the causal structure between greenhouse gases and global mean surface temperature (Stips et al., 2016) and the dynamical dependence between key observables and the Antarctic surface mass balance (Vannitsem et al., 2019). It constitutes an adequate framework to identify causal relationships between different climate variables.

In our study, we use the Liang-Kleeman information flow method to analyze the influence of several potential climate drivers on Arctic sea-ice area and volume, as well as the reverse impact of sea-ice area and volume on these drivers. We make use of the Swedish Meteorological and Hydrological Institute Large Ensemble (SMHI-LENS) to perform this analysis. We describe the data and methodology in Section 2, present our main results in Section 3, and provide our conclusions in Section 4.

2. Data and Methods

SMHI-LENS is one of the largest existing single-model large ensembles (Deser et al., 2020) using the Coupled Model Intercomparison Project 6 (CMIP6; Eyring et al. [2016]) forcing scenarios. It consists of 50 members realized with the global climate model EC-Earth3 (Döscher et al., 2022; Wyser et al., 2021). The atmosphere component, IFS cy36r4, has a horizontal resolution of ∼80 km, while the ocean component, NEMO3.6 (including the sea-ice model LIM3), has a horizontal resolution of ∼1°. The 50 ensemble members were started in 1970 from 50 different initial conditions using CMIP6 historical forcing and run until 2014. From 2015 until the end of the century, each member was run several times to take into account different greenhouse gas emission scenarios based on the Shared Socioeconomic Pathways (SSP; O'Neill et al. [2016]). More details about the SMHI-LENS protocol can be found in Wyser et al. (2021). In our study, we use the 50 members of SMHI-LENS over the historical period (1970-2014) and over the two most extreme SSP scenarios (2015-2100), that is, SSP1-1.9 and SSP5-8.5, corresponding to an increase in global mean near-surface temperature of less than 2°C and ∼6°C, respectively, between 1970 and 2100 (Wyser et al., 2021).

From the model monthly mean outputs, we compute Arctic sea-ice area (volume) based on the product of sea-ice concentration (sea-ice volume per area, respectively) in each grid point and grid-cell area, summed over all grid points north of 40°N. We focus on sea-ice area and volume in March and September, as these are months of maximum and minimum sea-ice area, respectively. We also compute six quantities that constitute potential atmospheric and ocean drivers of changes in Arctic sea ice based on the available literature: Arctic near-surface air temperature (Olonscheck et al., 2019), Arctic sea-surface temperature (SST, Docquier et al. [2021]), total Arctic Ocean heat transport (Onarheim et al., 2015), ocean heat transport at 70°N (Burgard & Notz, 2017), atmospheric heat transport at 70°N (Burgard & Notz, 2017), and Arctic Oscillation Index (AOI, Kretschmer et al. [2016]). We take the annual mean (January-December) for the first five quantities and the winter (January-March) average for AOI. Results of the method do not strongly depend on the starting month for computing the annual mean. In our study, by using annual means, we focus on the interannual time scale, and we acknowledge that the decadal time scale is not taken into account. More details about how the different quantities are computed are included in the Supporting Information.

In the high-emission scenario (SSP5-8.5), the ensemble mean March sea-ice area and volume decrease by 63% and 94%, respectively, across the 131 years of model simulation and the September sea ice completely disappears around 2060 (Figures 1a and 1b). This sea-ice loss is associated with an increase in Arctic near-surface temperature and SST of 18°C and 7°C, respectively (Figure 1c), an enhanced total Arctic Ocean heat transport of 180 TW (Figure 1d), and an increase in ocean heat transport at 70°N of 0.1 PW (Figure 1e) at the end of the century compared to 1970. The atmospheric heat transport at 70°N decreases by 0.3 PW across the twenty-first century (Figure 1e) and no significant change is detected for AOI due to large interannual variability (Figure 1f). In the low-emission scenario (SSP1-1.9), these changes are also apparent but with a much lower magnitude and a
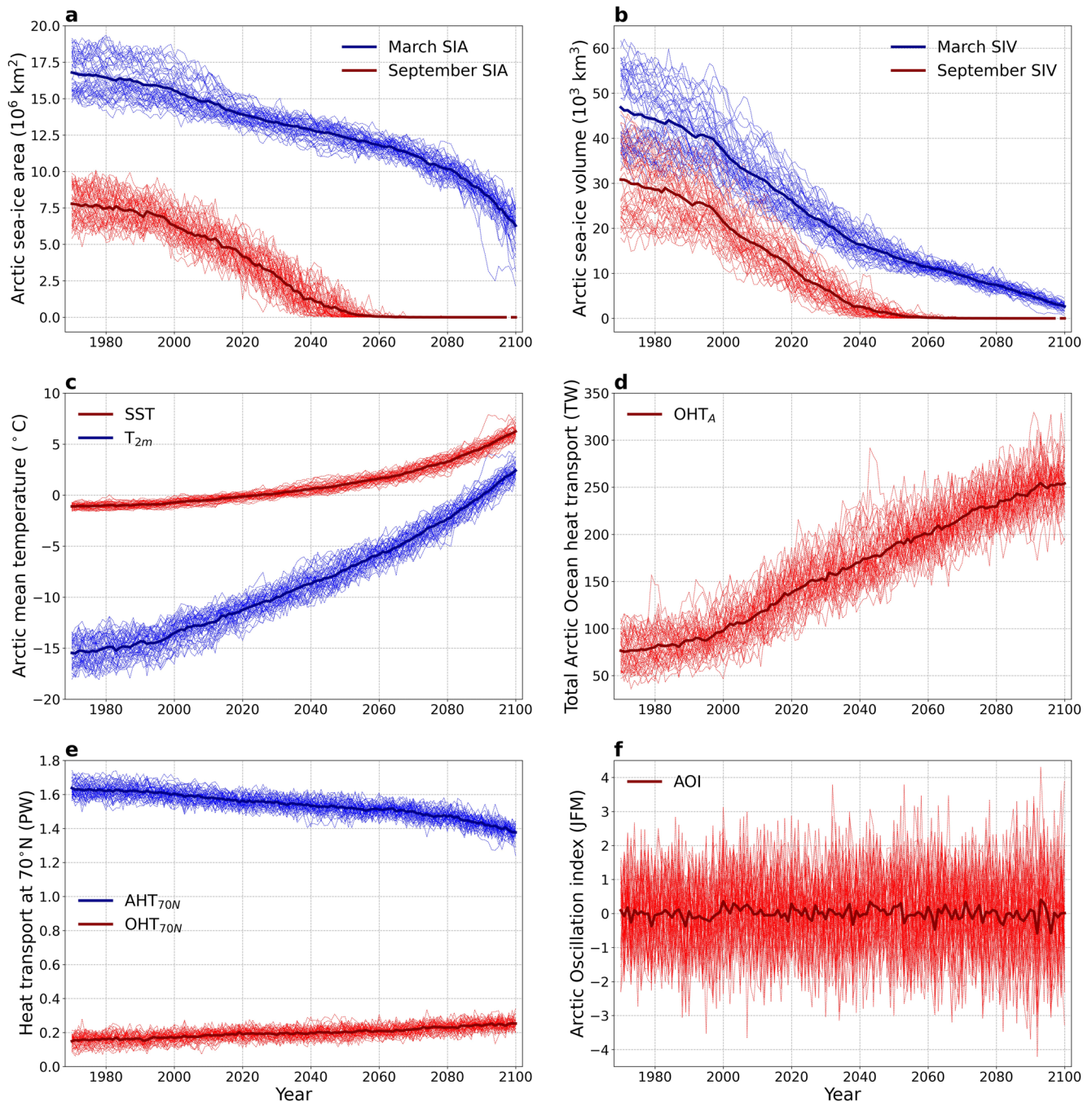
Figure 1. Time series of all considered variables for the 50 EC-Earth3 members (thin lines) and the ensemble mean (dark thick lines) over 1970-2100 (historical Coupled Model Intercomparison Project 6 run and SSP5-8.5 scenario). (a) March and September Arctic sea-ice area (SIA); (b) March and September Arctic sea-ice volume (SIV); (c) annual mean Arctic near-surface temperature (T_{2m}) and Arctic sea-surface temperature (SST); (d) annual mean total Arctic Ocean heat transport (OHT_A); (e) annual mean poleward ocean and atmospheric heat transports at 70°N (OHT_{70N} and AHT_{70N}); (f) winter (JFM) Arctic Oscillation index (AOI).

stabilization around the middle of the century (Figure S1). Especially, Arctic sea ice is still present in September and the ensemble mean September sea-ice area stabilizes at 1.8 million km^2 from around 2040 to 2100. In our study, we focus on SSP5-8.5 as the results between the two scenarios are relatively consistent in terms of transfer of information, but we also discuss differences between scenarios if they exist.

The absolute rate of information transfer from variable X_j to variable X_i is computed following Liang (2021):

$$T_{j \to i} = \frac{1}{\det \mathbf{C}} \cdot \sum_{k=1}^{d} \Delta_{jk} C_{k,di} \cdot \frac{C_{ij}}{C_{ii}}, \qquad (1)$$

where $\mathbf{C}$ is the covariance matrix, d is the number of variables ($d = 7$ in our case), Δ_{jk} are the cofactors of $\mathbf{C}$, $C_{k,di}$ is the sample covariance between all X_k and the Euler forward difference approximation of dX_i/dt (t is time), C_{ij} is the sample covariance between X_i and X_j, C_{ii} is the sample variance of X_i. When $T_{j \to i}$ is statistically different from 0, X_j has an influence on X_i, while if $T_{j \to i} = 0$ there is no influence. Statistical significance is computed via bootstrap resampling with replacement of all terms included in Equation 1 using 1,000 realizations. The rate of information transfer is normalized following Liang (2021) and is expressed in percent (see Supporting Information for more details).

We compute the transfer of information including the seven variables described above, where sea ice is either March sea-ice area, September sea-ice area, March sea-ice volume, or September sea-ice volume. This allows checking the role of sea-ice seasonality and the effect of using sea-ice thickness information or not. Two different methods for computing the rate of information transfer are used. In the first method, hereafter referred to as 'member analysis', the rate of information transfer is computed for each member separately. As the information flow method applies to stationary time series (see Supporting Information), we detrend each quantity before computing the rate of information transfer by removing the ensemble mean for each model member (Figure S2). Due to the limited amount of September sea ice after 2040 and as the two last decades show a strong acceleration in the reduction of March sea-ice area in the high-emission scenario (Figure 1a), we limit our analysis to 1970-2040 for September (71 data points for each member) and 1970-2080 for March (111 data points for each member). We take the ensemble mean rate of information transfer and check the statistical significance via the Fisher's method for multiple tests (Fisher [1992]; Figure 2). In the second method, hereafter referred to as 'time analysis', the rate of information transfer is computed for each range of 5 years separately (across the member space, resulting in 250 data points for each period of 5 years, except for the last period 2095-2100 including 6 years). The latter method allows checking the time evolution of the rate of information transfer between variables (Figures 3 and 4). Having 50 ensemble members allows to reduce the uncertainty related to internal variability (Jahn et al., 2016) for the member analysis, and brings a sufficient number of data points for the time analysis.

3. Results

### 3.1. Member Analysis: Rate of Information Transfer Across the Full Time Series

We first look at drivers of Arctic sea-ice variability over the whole time period. Figure 2 provides a summary of results from the member analysis as matrices of the ensemble mean relative rate of information transfer and correlation coefficient between March/September sea-ice area and its potential drivers based on SSP5-8.5. The self-influence of variables (shown in the matrix diagonals) is the largest compared to other influences ($|\tau|$ ranging between 36% and 63%; Figures 2a and 2c). In the current framework, a self-influence means that the dynamics of the variable state depend on the variable state itself (Liang, 2021).

Beside these self-influences, there is a two-way significant information transfer between March sea-ice area on the one hand, and near-surface temperature, Arctic SST and Arctic Ocean heat transport on the other hand, as well as a significant influence of ocean heat transport at 70°N on March sea-ice area (Figure 2a). The causal links are stronger from March sea-ice area to near-surface temperature ($|\tau| = 13\%$), to SST ($|\tau| = 9\%$), and to Arctic Ocean heat transport ($|\tau| = 9\%$; first row in Figure 2a), than the reverse (first column in Figure 2a). This suggests that recent and future changes in March sea-ice area have a strong impact on Arctic temperatures (both at the sea surface and air surface) and ocean heat transport. The influence of sea-ice area on sea-surface and air temperatures is strongly linked to the ice-albedo feedback (Andry et al., 2017; Massonnet et al., 2018; Wunderling et al., 2020). One potential mechanism by which ocean heat transport is affected by sea-ice changes is the following: the decline in Arctic sea ice leads to smaller ice export through Fram Strait and to an increase in Greenland Sea salinity. The latter lower sea-surface height and strengthens the cyclonic gyre circulation in the Nordic Seas, resulting in increased volume and heat transport of Atlantic water into the Arctic Ocean through Fram Strait (Wang et al., 2020). Additionally, correlation coefficients are negative between March sea-ice area and Arctic near-surface temperature ($R = -0.79$), Arctic SST ($R = -0.75$), and Arctic Ocean heat transport ($R = -0.59$; Figure 2b). Thus, combining the relative rates of information transfer and correlation coefficients, we can infer
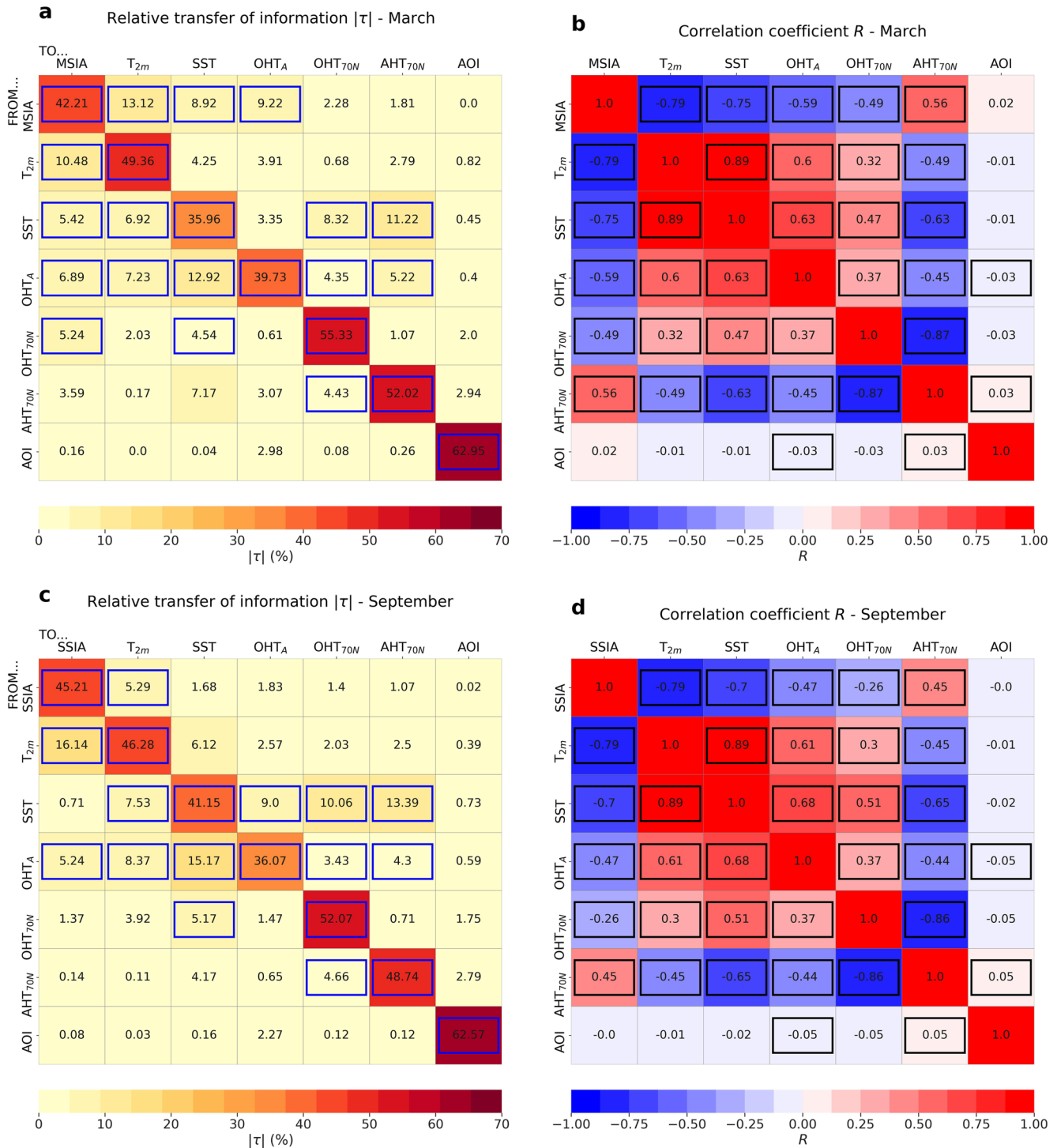
Figure 2. Matrices of EC-Earth3 ensemble mean (a, c) relative rate of information transfer τ (in absolute value; unit: %) and (b, d) correlation coefficient R between (a, b) March Arctic sea-ice area (MSIA, 1970-2080), (c, d) September sea-ice area (SSIA, 1970-2040) and the six drivers for which acronym definitions are provided in the caption of Figure 1, based on historical Coupled Model Intercomparison Project 6 run and SSP5-8.5 scenario. The highlighted elements are significant at the 5% level based on Fisher's method for multiple tests.

that the ongoing decrease in March sea-ice area leads to larger SST, larger near-surface temperature, and larger ocean heat transport in the Arctic. Although slightly weaker, a similar conclusion can be drawn for the influence of air temperature, SST and ocean heat transport on March sea-ice area.
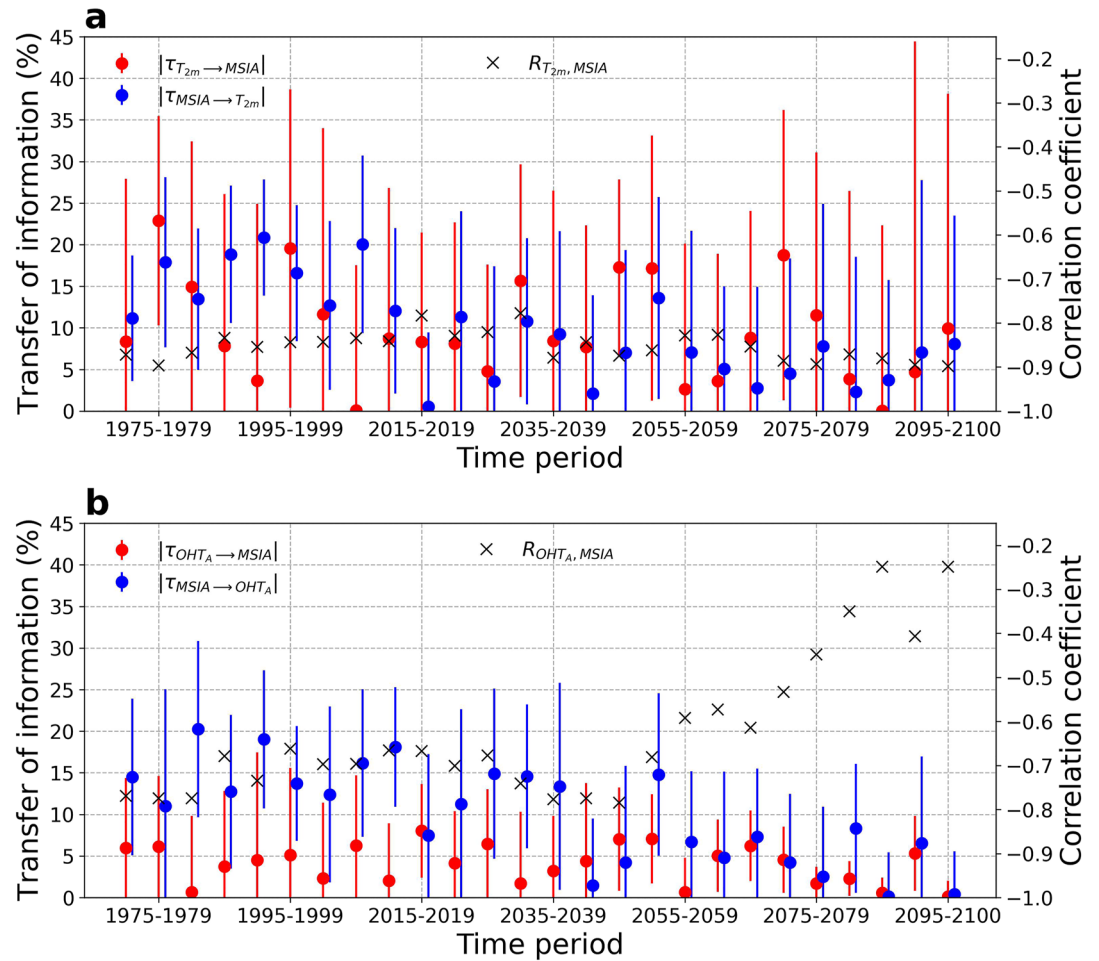
Figure 3. Time evolution of the relative rate of information transfer τ (in absolute value; left axis) and correlation coefficient R (right axis) for each period of 5 years between 1970 and 2100 (historical Coupled Model Intercomparison Project 6 run and SSP5-8.5 scenario), computed over the 50 EC-Earth3 members. (a) Transfer of information from annual mean Arctic near-surface air temperature (T_{2m}) to March Arctic sea-ice area (MSIA) (red circles), from MSIA to T_{2m} (blue circles), and correlation coefficient between T_{2m} and MSIA (black crosses). (b) Transfer of information from annual mean total Arctic Ocean heat transport (OHT_A) to MSIA (red circles), from MSIA to OHT_A (blue circles), and correlation coefficient between OHT_A and MSIA (black crosses). The error bars show the 95% confidence intervals for τ using bootstrap with replacement.

By contrast with March, September sea-ice area has a significant influence only on near-surface temperature (but this is relatively reduced, i.e., $|\tau| = 5\%$; Figure 2c). Also, while changes in March sea-ice area are driven by changes in air and sea-surface temperature, as well as ocean heat transport (Figure 2a), changes in September sea-ice area primarily come from changes in near-surface temperature ($|\tau| = 16\%$; Figure 2c). Arctic sea-ice area is more than twice larger in March compared to September (Figure 1a), and sea ice is present in March in (or close to) regions where large increases in ocean heat transport and SST have been reported in the past years, such as the Barents Sea (Arthun et al., 2012), Laptev Sea (Polyakov et al., 2017), and Chukchi Sea (Serreze et al., 2019). Thus, the role of a warming ocean and enhanced ocean heat transport on sea ice is greater in March compared to September. As sea ice is much more confined to the central Arctic in September, the primary driver of September sea-ice area decrease in the past and future years is the air temperature.

Results from the member analysis are relatively similar for the weak greenhouse gas emission scenario (SSP1-1.9), with a larger influence of March sea-ice area on Arctic near-surface temperature and ocean heat transport than the reverse, a larger impact of air temperature on the sea-ice area in September than in March, and a stronger causal link from the ocean (SST) to the sea-ice area in March (Figure S3). An exception in SSP1-1.9, compared to SSP5-8.5, is that there is no significant information transfer from air temperature and Arctic Ocean heat transport to March sea-ice area. When taking sea-ice volume instead of sea-ice area, the influence of near-surface
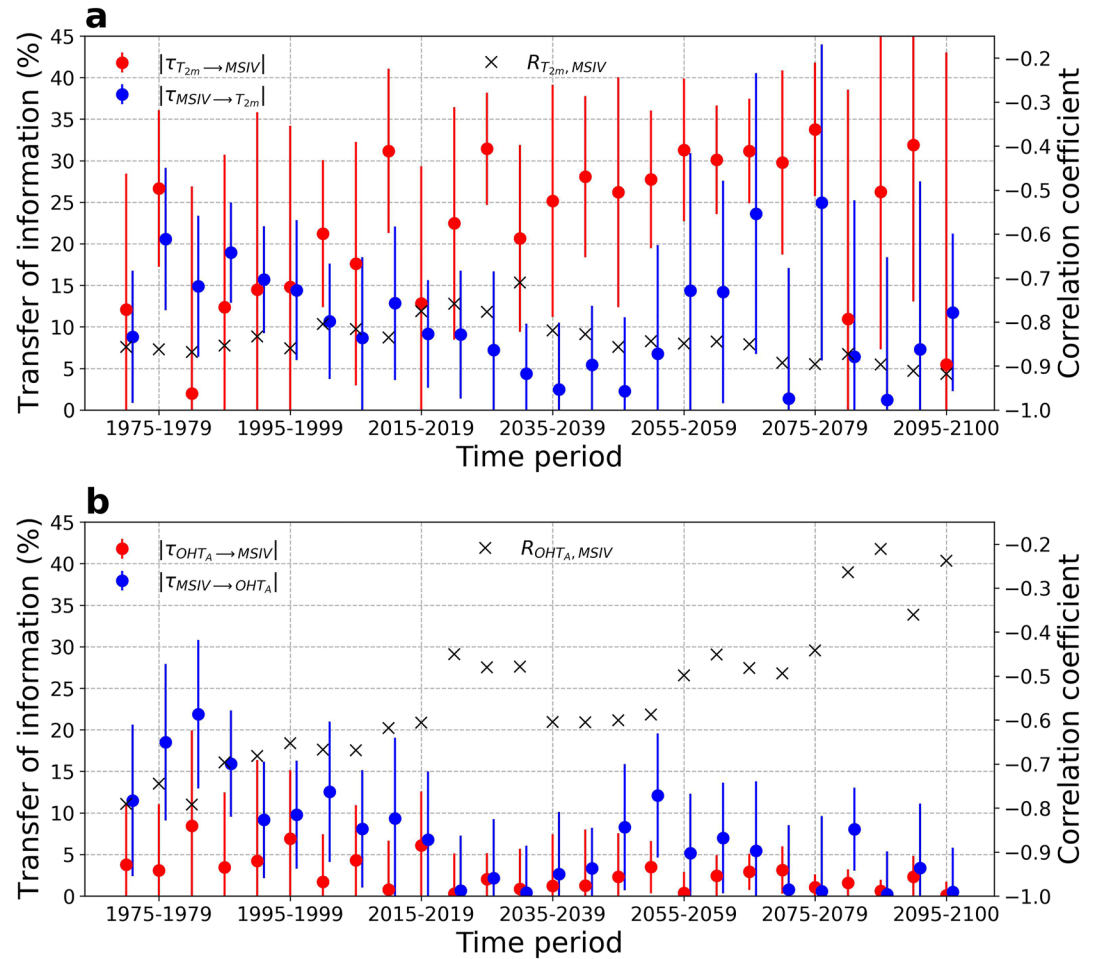
Figure 4. Time evolution of relative rate of information transfer τ (in absolute value; left axis) and correlation coefficient R (right axis) for each period of 5 years between 1970 and 2100 (historical Coupled Model Intercomparison Project 6 run and SSP5-8.5 scenario), computed over the 50 EC-Earth3 members. (a) Transfer of information from annual mean Arctic near-surface air temperature (T_{2m}) to March Arctic sea-ice volume (MSIV) (red circles), from MSIV to T_{2m} (blue circles), and correlation coefficient between T_{2m} and MSIV (black crosses). (b) Transfer of information from annual mean total Arctic Ocean heat transport (OHT_A) to MSIV (red circles), from MSIV to OHT_A (blue circles), and correlation coefficient between OHT_A and MSIV (black crosses). The error bars show the 95% confidence intervals for τ using bootstrap with replacement.

temperature and SST on March sea-ice volume becomes larger than the reverse in the two emission scenarios (Figures S4a and S5a). This suggests that temperature changes at the surface of the ocean and above greatly affect sea-ice thickness. In September, near-surface temperature constitutes by far the largest driver of sea-ice volume, similar to the sea-ice area, but during this month sea-ice volume also affects SST and Arctic Ocean heat transport (Figures S4c and S5c), while it is not the case for the sea-ice area (Figures 2c and S3c in Supporting Information S1). Thus, changes in sea-ice thickness play an important role in driving changes in ocean temperature and heat transport.

For the two scenarios, no causal influence is detected between sea-ice area and volume in March and September on the one hand, and AOI on the other hand. While no influence of sea-ice area and volume on the ocean and atmospheric heat transport at 70°N is found in any of the two scenarios, ocean heat transport at 70°N appears to cause changes in March sea-ice area (Figures 2a-S3a in Supporting Information S1), in agreement with results found in Burgard and Notz (2017) and Docquier et al. (2019), and atmospheric heat transport has an influence on March sea-ice volume (Figures S4a-S5a). Interestingly, a significantly positive correlation appears between March sea-ice area and atmospheric heat transport at 70°N ($R = 0.56$; Figure 2b), but no significant transfer of information exists (Figure 2a). This suggests that an external driver causes concomitant changes in the sea-ice area and atmospheric heat transport, while these two quantities do not influence each other. The main suspect is

SST as it influences both variables: an increase in SST leads to the lower sea-ice area and lower atmospheric heat transport at 70°N (Figures 2a and 2b). This further demonstrates that correlation does not mean causation and shows the strength of the Liang-Kleeman information flow method (Liang, 2014).

3.2. Time Analysis: Evolution of the Rate of Information Transfer

Based on the previous member analysis (Section 3.1), near-surface temperature, SST and Arctic Ocean heat transport constitute the most important drivers of changes in Arctic sea ice, and conversely. For the time analysis, we focus on the cause-effect relationships between near-surface air temperature and Arctic Ocean heat transport on the one hand, and Arctic sea-ice area and volume on the other hand. We do not consider SST as this quantity is somewhat integrated into ocean heat transport and is thus redundant. The goal of the time analysis is to clarify the modifications in the rate of information transfer under climate change.

The correlation coefficient between March Arctic sea-ice area and Arctic near-surface temperature stays relatively constant through the whole time period with large negative values ($R = -0.75$ to -0.9; Figure 3a), in agreement with previous studies (e.g., Olonscheck et al., 2019). The relative rate of information transfer from near-surface temperature to March sea-ice area shows a large 5-year variability, with a peak in 1975–1979 ($|\tau| \approx 23\%$) and four additional 5-year periods having a significant influence (Figure 3a). The number of periods with a significant rate of information transfer from March sea-ice area to near-surface temperature is twice more important (i.e., 11 periods) than the reverse influence (Figure 3a), which confirms previous results from the member analysis (Section 3.1). Additionally, no significant influence of March sea-ice area on near-surface temperature remains after 2050, while one 5-year period shows an influence of temperature on sea-ice area after 2050 (Figure 3a). In September, the rate of information transfer from near-surface temperature to sea-ice area is generally larger than from sea-ice area to temperature, and peaks in 2025–2029 before decreasing (Figure S6a).

As for the information transfer from March sea-ice area to near-surface temperature, the rate of information transfer from March sea-ice area to the Arctic Ocean heat transport generally decreases over time, with almost no significant influence after 2050 (Figure 3b). For the reverse transfer of information from ocean heat transport to Arctic sea-ice area, eight periods are significant, with five periods after 2050, but with relatively low values ($|\tau| = 6\text{-}7\%$). Year 2050 also marks a threshold after which the correlation coefficient between March sea-ice area and ocean heat transport starts decreasing from $R \approx -0.7$ on average for 1970-2049 to $R = -0.25$ in 2095–2100 (Figure 3b). Thus, as the sea-ice area becomes smaller, the two-way influence between sea-ice area and near-surface temperature and ocean heat transport becomes weaker. This is also the case in September with a decrease starting earlier on due to lower sea-ice area during that month (Figure S6b). Results are qualitatively similar in the low greenhouse gas emission scenario (Figures S7-S8).

Contrarily to the rate of information transfer from near-surface temperature to March sea-ice area, the information transfer from near-surface temperature to March sea-ice volume remains strong almost until the end of the century, with values of $|\tau|$ between ~10% and 35% (Figure 4a). This means that the increase in air temperature leads to a decrease in sea-ice volume until the end of the century. This result is counter-intuitive as sea ice is getting thinner and sea-ice area and volume are expected to behave in a more similar way across the twenty-first century. Changes in March sea-ice volume also influence changes in near-surface temperature, but with lower values of information transfer than the reverse influence and a progressive decrease across time (Figure 4a). In September, the information transfer is also generally larger from near-surface temperature to sea-ice volume than the reverse, except at the beginning of the model simulation (1970-1995; Figure S9a).

As for the March sea-ice area - ocean heat transport relationship, the correlation coefficient between March sea-ice volume and ocean heat transport decreases over time (Figure 4b). This coincides with a decrease over time in the influence of March sea-ice volume on ocean heat transport. The transfer of information from ocean heat transport to March sea-ice volume stays relatively low through the whole twenty-first century, with only three 5-year periods showing a significant transfer of information (Figure 4b). Results are qualitatively similar when considering September sea-ice volume (Figure S9b), as well as the SSP1-1.9 scenario (Figures S10-S11). The use of slightly smaller (3–4 years) or larger (10 years) periods does not change our key results.

4. Conclusions and Perspectives

In our study, we have applied for the first time the Liang-Kleeman information flow method to the analysis of causal influences between Arctic sea-ice area and volume and their potential drivers using SMHI-LENS (50 members simulated with EC-Earth3). We found that the recent and future changes in Arctic sea-ice area and volume are mainly driven by near-surface air temperature, sea-surface temperature, and ocean heat transport, in agreement with previous studies (Olonscheck et al., 2019; Onarheim et al., 2015). More surprisingly, the reverse influence of sea-ice area and volume on temperature and ocean heat transport also exists and is sometimes larger than the reverse influence depending on the quantity (sea-ice area or volume) and the month of the year (March or September). This two-way influence indicates that the current decrease in Arctic sea-ice area and volume is not solely related to air temperature and, consequently to greenhouse gas emissions (Notz & Stroeve, 2016), but is also potentially driven by feedback mechanisms between sea ice, the atmosphere and the ocean (Goosse et al., 2018; Pithan & Mauritsen, 2014).

Our results also show a progressive loss of influence of sea-ice area and volume on air temperature and ocean heat transport through the twenty-first century on the one hand. This indicates that interactions between sea ice, the atmosphere, and the ocean, especially the ice-albedo feedback (Wunderling et al., 2020), become weaker as sea-ice area decreases. On the other hand, the rate of information transfer from air temperature to September Arctic sea-ice area and volume (in both March and September) remains more constant through time and relatively large. This suggests that changes in near-surface temperature have a long-lasting effect on September sea-ice area and March and September sea-ice volume. Identifying the thermo-dynamical mechanisms causing these differences in directional dependence across time should be addressed in the future. This could be achieved via an analysis of the exact processes by which sea ice melts and refreezes, combined with the Liang-Kleeman information flow method. Finally, as sea-ice changes are not spatially uniform (Arthun et al., 2021; Onarheim et al., 2018), extending this analysis to different regions of the Arctic could also provide more insight into the spatial variability of the information transfer between Arctic sea ice and its drivers.

Data Availability Statement

Model data from EC-Earth3 SMHI-LENS (Wyser et al., 2021) are available on the Earth System Grid Federation (ESGF) nodes (https://esgf-node.llnl.gov/search/cmip6) via a search for 'Source ID' = EC-Earth3 and 'Variant Label' = r101i1p1f1 to r150i1p1f1. The Python scripts to produce the figures of this article are available on Zenodo: https://zenodo.org/record/6375655 (Docquier, 2022).

References

Andry, O., Bintanja, R., & Hazeleger, W. (2017). Time-dependent variations in the Arctic's surface albedo feedback and the link to seasonality in sea ice. *Journal of Climate*, *30*(1), 393–410. https://doi.org/10.1175/JCLI-D-15-0849.1

Arthun, M., Eldevik, T., Smedsrud, L. H., Skagseth, O., & Ingvaldsen, R. B. (2012). Quantifying the influence of Atlantic heat on Barents Sea ice variability and retreat. *Journal of Climate*, *25*(13), 4736–4743. https://doi.org/10.1175/JCLI-D-11-00466.1

Arthun, M., Onarheim, I. H., Dorr, J., & Eldevik, T. (2021). The seasonal and regional transition to an ice-free Arctic. *Geophysical Research Letters*, *48*(1), e2020GL090825. https://doi.org/10.1029/2020GL090825

Auclair, G., & Tremblay, B. (2018). The role of ocean heat transport in rapid sea ice declines in the Community Earth System Model Large Ensemble. *Journal of Geophysical Research*, *123*(12), 8941–8957. https://doi.org/10.1029/2018JC014525

Burgard, C., & Notz, D. (2017). Drivers of Arctic Ocean warming in CMIP5 models. *Geophysical Research Letters*, *44*(9), 4263–4271. https://doi.org/10.1002/2016GL072342

Carmack, E., Polyakov, I., Padman, L., Fer, I., Hunke, E., Hutchings, J., et al. (2015). Toward quantifying the increasing role of oceanic heat in sea ice loss in the new Arctic. *Bulletin of the American Meteorological Society*, *96*(12), 2079–2105. https://doi.org/10.1175/BAMS-D-13-00177.1

Deser, C., Lehner, F., Rodgers, K. B., Ault, T., Delworth, T. L., DiNezio, P. N., et al. (2020). Insights from Earth system model initial-condition large ensembles and future prospects. *Nature Climate Change*, *10*, 277–286. https://doi.org/10.1038/s41558-020-0731-2

Deza, J. I., Barreiro, M., & Masoller, C. (2015). Assessing the direction of climate interactions by means of complex networks and information theoretic tools. *Chaos*, *25*, 033105. https://doi.org/10.1063/1.4914101

Ding, Q., Schweiger, A., L'Heureux, M., Battisti, D. S., Po-Chedley, S., Johnson, N. C., et al. (2017). Influence of high-latitude atmospheric circulation changes on summertime Arctic sea ice. *Nature Climate Change*, *7*, 289–295. https://doi.org/10.1038/nclimate3241

Docquier, D. (2022). Liang Index to quantify causal links between Arctic sea ice and its drivers (v2.1). *Zenodo*. https://doi.org/10.5281/ zenodo.6375655

Docquier, D., Grist, J. P., Roberts, M. J., Roberts, C. D., Semmler, T., Ponsoni, L., et al. (2019). Impact of model resolution on Arctic sea ice and North Atlantic Ocean heat transport. *Climate Dynamics*, *53*, 4989–5017. https://doi.org/10.1007/s00382-019-04840-y

Docquier, D., & Koenigk, T. (2021). Observation-based selection of climate models projects Arctic ice-free summers around 2035. *Communications Earth & Environment*, *2*(144). https://doi.org/10.1038/s43247-021-00214-7

Docquier, D., Koenigk, T., Fuentes-Franco, R., Karami, M. P., & Ruprich-Robert, Y. (2021). Impact of ocean heat transport on the Arctic sea-ice decline: A model study with EC-Earth3. *Climate Dynamics*, *56*, 1407–1432. https://doi.org/10.1007/s00382-020-05540-8

Döscher, R., Acosta, M., Alessandri, A., Anthoni, P., Arsouze, T., Bergman, T., et al. (2022). The EC-Earth3 Earth system model for the Coupled Model Intercomparison Project 6. *Geoscientific Model Development*, *15*, 2973–3020. https://doi.org/10.5194/gmd-15-2973-2022

Eyring, V., Bony, S., Meehl, G. A., Senior, C. A., Stevens, B., Stouffer, R. J., & Taylor, K. E. (2016). Overview of the Coupled Model Intercomparison Project Phase 6 (CMIP6) experimental design and organization. *Geoscientific Model Development*, *9*, 1937–1958. https://doi.org/10.5194/gmd-9-1937-2016

Fisher, R. A. (1992). Statistical methods for research workers. In S.Kotz, & N.L.Johnson (Eds.), *Breakthroughs in Statistics. Springer series in Statistics (Perspectives in Statistics)*: Springer. https://doi.org/10.1007/978-1-4612-4380-9_6

Goosse, H., Kay, J. E., Armour, K. C., Bodas-Salcedo, A., Chepfer, H., Docquier, D., et al. (2018). Quantifying climate feedbacks in polar regions. *Nature Communications*, *9*(1919), 1–13. https://doi.org/10.1038/s41467-018-04173-0

Granger, C. W. (1969). Investigating causal relations by econometric models and cross-spectral methods. *Econometrica*, *37*(3), 424–438. https://doi.org/10.2307/1912791

Harries, D., & O'Kane, T. J. (2021). Dynamic Bayesian networks for evaluation of Granger causal relationships in climate reanalyses. *Journal of Advances in Modeling Earth Systems*, *13*(5), e2020MS002442. https://doi.org/10.1029/2020MS002442

IPCC. (2019). Summary for Policymakers. In H.-O.Pörtner, D.C.Roberts, V.Masson-Delmotte, P.Zhai, M.Tignor, E.Poloczanska, K.Mintenbeck, A.Alegria, M.Nicolai, A.Okem, J.Petzold, B. Rama, & N.M.Weyer (Eds.), *IPCC Special Report on the Ocean and Cryosphere in a Changing Climate*: Cambridge University Press.

Jahn, A., Kay, J. E., Holland, M. M., & Hall, D. M. (2016). How predictable is the timing of a summer ice-free Arctic? *Geophysical Research Letters*, *43*(17), 9113–9120. https://doi.org/10.1002/2016GL070067

Krakovska, A., Jakubik, J., Chvostekova, M., Coufal, D., Jajcay, N., & Palus, M. (2018). Comparison of six methods for the detection of causality in a bivariate time series. *Physical Review E*, *97*(4), 042207. https://doi.org/10.1103/PhysRevE.97.042207

Kretschmer, M., Coumou, D., Donges, J. F., & Runge, J. (2016). Using causal effect networks to analyze different Arctic drivers of midlatitude winter circulation. *Journal of Climate*, *29*(11), 4069–4081. https://doi.org/10.1175/JCLI-D-15-0654.1

Kwok, R. (2018). Arctic sea ice thickness, volume, and multiyear ice coverage: Losses and coupled variability (1958-2018). *Environmental Research Letters*, *13*(10), 105005. https://doi.org/10.1088/1748-9326/aae3ec

Liang, X. S. (2014). Unraveling the cause-effect relation between time series. *Physical Review E*, *90*(5), 052150. https://doi.org/10.1103/PhysRevE.90.052150

Liang, X. S. (2021). Normalized multivariate time series causality analysis and causal graph reconstruction. *Entropy*, *23*(6), 679. https://doi.org/10.3390/e23060679

Liang, X. S., & Kleeman, R. (2005). Information transfer between dynamical system components. *Physical Review Letters*, *95*(24), 244101. https://doi.org/10.1103/PhysRevLett.95.244101

Lindsay, R., & Schweiger, A. (2015). Arctic sea ice thickness loss determined using subsurface, aircraft, and satellite observations. *The Cryosphere*, *9*, 269–283. https://doi.org/10.5194/tc-9-269-2015

Massonnet, F., Vancoppenolle, M., Goosse, H., Docquier, D., Fichefet, T., & Blanchard-Wrigglesworth, E. (2018). Arctic sea-ice change tied to its mean state through thermodynamic processes. *Nature Climate Change*, *8*, 599–603. https://doi.org/10.1038/s41558-018-0204-z

Mosedale, T. J., Stephenson, D. B., Collins, M., & Mills, T. C. (2006). Granger causality of coupled climate processes: Ocean feedback on the North Atlantic Oscillation. *Journal of Climate*, *19*(7), 1182–1194. https://doi.org/10.1175/JCLI3653.1

Notz, D., & Stroeve, J. (2016). Observed Arctic sea-ice loss directly follows anthropogenic CO_2 emission. *Science*, *354*(6313), 747–750. https://doi.org/10.1126/science.aag2345

Olonscheck, D., Mauritsen, T., & Notz, D. (2019). Arctic sea-ice variability is primarily driven by atmospheric temperature fluctuations. *Nature Geoscience*, *12*, 430–434. https://doi.org/10.1038/s41561-019-0363-1

Onarheim, I. H., Eldevik, T., Arthun, M., Ingvaldsen, R. B., & Smedsrud, L. H. (2015). Skillful prediction of Barents Sea ice cover. *Geophysical Research Letters*, *42*(13), 5364–5371. https://doi.org/10.1002/2015GL064359

Onarheim, I. H., Eldevik, T., Smedsrud, L. H., & Stroeve, J. C. (2018). Seasonal and regional manifestation of Arctic sea ice loss. *Journal of Climate*, *31*(12), 4917–4932. https://doi.org/10.1175/JCLI-D-17-0427.1

O'Neill, B. C., Tebaldi, C., vanVuuren, D. P., Eyring, V., Friedlingstein, P., Hurtt, G., et al. (2016). The Scenario Model Intercomparison Project (ScenarioMIP) for CMIP6. *Geoscientific Model Development*, *9*, 3461–3482. https://doi.org/10.5194/gmd-9-3461-2016

Pithan, F., & Mauritsen, T. (2014). Arctic amplification dominated by temperature feedbacks in contemporary climate models. *Nature Geoscience*, *7*, 181–184. https://doi.org/10.1038/NGEO2071

Polyakov, I. V., Pnyushkov, A. V., Alkire, M. B., Ashik, I. M., Baumann, T. M., Carmack, E. C., et al. (2017). Greater role for Atlantic inflows on sea-ice loss in the Eurasian basin of the Arctic Ocean. *Science*, *356*(6335), 285–291. https://doi.org/10.1126/science.aai8204

Runge, J., Bathiany, S., Bollt, E., Camps-Valls, G., Coumou, D., Deyle, E., et al. (2019). Inferring causation from time series in Earth system sciences. *Nature Communications*, *10*, 2553. https://doi.org/10.1038/s41467-019-10105-3

Sando, A. B., Gao, Y., & Langehaug, H. R. (2014). Poleward ocean heat transports, sea ice processes, and Arctic sea ice variability in NorESM1-M simulations. *Journal of Geophysical Research*, *119*(3), 2095–2108. https://doi.org/10.1002/2013JC009435

Schweiger, A. J., Wood, K. R., & Zhang, J. (2019). Arctic sea ice volume variability over 1901-2010: A model-based reconstruction. *Journal of Climate*, *32*(15), 4731–4752. https://doi.org/10.1175/JCLI-D-19-0008.1

Serreze, M. C., Barrett, A. P., Crawford, A. D., & Woodgate, R. A. (2019). Monthly variability in Bering Strait oceanic volume and heat transports, links to atmospheric circulation and ocean temperature, and implications for sea ice conditions. *Journal of Geophysical Research*, *124*(12), 9317–9337. https://doi.org/10.1029/2019JC015422

SIMIP Community. (2020). Arctic sea ice in CMIP6. *Geophysical Research Letters*, *47*(10), e2019GL086749. https://doi.org/10.1029/2019GL086749

Stips, A., Macias, D., Coughlan, C., Garcia-Gorriz, E., & Liang, X. S. (2016). On the causal structure between CO_2 and global temperature. *Scientific Reports*, *6*, 21691. https://doi.org/10.1038/srep21691

Stroeve, J., & Notz, D. (2018). Changing state of Arctic sea ice across all seasons. *Environmental Research Letters*, *13*(10), 103001. https://doi.org/10.1088/1748-9326/aade56

Sugihara, G., May, R., Ye, H., Hsieh, C.-H., Deyle, E., Fogarty, M., & Munch, S. (2012). Detecting causality in complex ecosystems. *Science*, *338*(6106), 496–500. https://doi.org/10.1126/science.1227079

Swart, N. C., Fyfe, J. C., Hawkins, E., Kay, J. E., & Jahn, A. (2015). Influence of internal variability on Arctic sea-ice trends. *Nature Climate Change*, *5*, 86–89. https://doi.org/10.1038/nclimate2483

Tsonis, A. A., Deyle, E. R., May, R. M., Sugihara, G., Swanson, K., Verbeten, J. D., & Wang, G. (2015). Dynamical evidence for causality between galactic cosmic rays and interannual variation in global temperature. *Proceedings of the National Academy of Sciences of the United States of America*, *112*(11), 3253–3256. https://doi.org/10.1073/pnas.1420291112

Vannitsem, S., Dalaiden, Q., & Goosse, H. (2019). Testing for dynamical dependence: Application to the surface mass balance over Antarctica. *Geophysical Research Letters*, *46*(21), 12125–12135. https://doi.org/10.1029/2019GL084329

Vannitsem, S., & Ekelmans, P. (2018). Causal dependences between the coupled ocean–atmosphere dynamics over the tropical Pacific, the North Pacific and the North Atlantic. *Earth System Dynamics*, *9*, 1063–1083. https://doi.org/10.5194/esd-9-1063-2018

Wang, Q., Wekerle, C., Wang, X., Danilov, S., Koldunov, N., Sein, D., et al. (2020). Intensification of the Atlantic water supply to the Arctic Ocean through Fram Strait induced by Arctic sea ice decline. *Geophysical Research Letters*, *47*(3), e2019GL086682. https://doi.org/10.1029/2019GL086682

Wunderling, N., Willeit, M., Donges, J. F., & Winkelmann, R. (2020). Global warming due to loss of large ice masses and Arctic summer sea ice. *Nature Communications*, *11*(5177). https://doi.org/10.1038/s41467-020-18934-3

Wyser, K., Koenigk, T., Fladrich, U., Fuentes-Franco, R., Karami, M. P., & Kruschke, T. (2021). The SMHI Large Ensemble (SMHI-LENS) with EC-Earth3.3.1. *Geoscientific Model Development*, *14*, 4781–4796. https://doi.org/10.5194/gmd-14-4781-2021

References From the Supporting Information

Lavergne, T., Sorensen, A. M., Kern, S., Tonboe, R., Notz, D., Aaboe, S., et al. (2019). Version 2 of the EUMETSAT OSI SAF and ESA CCI sea-ice concentration climate data records. *The Cryosphere*, *13*, 49–78. https://doi.org/10.5194/tc-13-49-2019

van der Linden, E. C., Le Bars, D., Bintanja, R., & Hazeleger, W. (2019). Oceanic heat transport into the Arctic under high and low CO2 forcing. *Climate Dynamics*, *53*, 4763–4780. https://doi.org/10.1007/s00382-019-04824-y

Tsubouchi, T., Vage, K., Hansen, B., Larsen, K. M. H., Osterhus, S., Johnson, C., et al. (2021). Increased ocean heat transport into the Nordic Seas and Arctic Ocean over the period 1993–2016. *Nature Climate Change*, *11*, 21–26. https://doi.org/10.1038/s41558-020-00941-3

Zhang, J., Sheng, Z., Ma, Y., He, Y., Zuo, X., & He, M. (2021). Analysis of the positive Arctic Oscillation Index event and its influence in the winter and spring of 2019/2020. *Frontiers in Earth Science*, *8*(580601), 1–17. https://doi.org/10.3389/feart.2020.580601